Available online at www.sciencedirect.com
SCIENCE DIRECT
Polymer 47 (2006) 4581–4587
polymer
www.elsevier.com/locate/polymer

Double-responsive core–shell–corona micelles from self-assembly of diblock copolymer of poly(*t*-butyl acrylate-*co*-acrylic acid)-*b*-poly(*N*-isopropylacrylamide)

Guiying Li, Linqi Shi *, Yingli An, Wangqing Zhang, Rujiang Ma

Key Laboratory of Functional Polymer Materials, Ministry of Education, Institute of Polymer Chemistry, Nankai University, Tianjin 300071, China

Received 17 February 2006; received in revised form 3 April 2006; accepted 23 April 2006
Available online 18 May 2006

Abstract

Self-assembly of poly(*t*-butyl acrylate-*co*-acrylic acid)-*b*-poly(*N*-isopropylacrylamide) [P(*t*BA-*co*-AA)-*b*-PNIPAM], which was obtained from part hydrolysis of P*t*BA-*b*-PNIPAM synthesized by sequential atom transfer radical polymerization (ATRP) was studied. Thermo- and pH-responsive core–shell–corona (CSC) micelles with different structures were formed from (P*t*BA-*co*-PAA)-*b*-PNIPAM in aqueous solution. At pH 5.8 and 25 °C, the block copolymer self-assembled into spherical core–shell micelles with hydrophobic P*t*BA segments as the core, hydrophilic PAA/PNIPAM segments as the mixed shell. Increasing temperatures, core–shell micelles converted into CSC micelles with P*t*BA as the core, collapsed PNIPAM as the shell and soluble PAA as the corona. Moreover, decreasing pH at 25 °C, PAA chains collapsed onto the core resulting in CSC micelles with P*t*BA as the core, PAA as the shell and PNIPAM as the corona.

Keywords: Poly(*t*-butyl acrylate-*co*-acrylic acid)-*b*-poly(*N*-isopropylacrylamide); Stimuli-responsive; Micelles

1. Introduction

Stimuli-responsive copolymers whose behaviors depend strongly on the external chemical and physical stimuli, such as temperature, pH, ionic strength, light and electric field, have attracted increasing research attentions for their wide range of applications in gene and drug delivery, chemical and biological sensors, etc. [1–9]. Poly(*N*-isopropylacrylamide) (PNIPAM) is one of the most studied thermo-responsive polymers that exhibits a lower critical solution temperature (LCST) in water around 32 °C [10,11]. Below the LCST, PNIPAM is soluble in aqueous solution, while above the LCST, PNIPAM shows a sharp phase transition and precipitates. It is this unusual phase transition temperature and its related solution properties that have attracted great theoretical and technological interests [12–17]. The pH-responsive polymers can respond to pH changes to adjust their morphology and conformation due to the protonation–deprotonation equilibrium in aqueous solution [18].

Block copolymers containing both of thermo- and pH-responsive segments can respond to combined external stimuli [19–22]. Armes et al. reported a diblock copolymer of poly(propylene oxide)-*b*-poly(2-(diethylamino)ethyl methacrylate), which dissolved molecularly in cold aqueous solution and self-assembled into PPO-core micelles or DEA-core micelles by adjusting pH and temperature [21]. Muller et al. studied the self-assembly of thermo- and pH-responsive PNIPAM-*b*-PAA diblock copolymer in water [22]. All these studies focused on the reversible changes of core–shell micelles.

Apart from core–shell micelles [23,24], core–shell–corona (CSC) micelles that have more defined structures have been extensively studied. Usually, CSC micelles are prepared from amphiphilic ABC triblock copolymers [25–29] or mixtures of AB block copolymer and C homopolymer or two diblock copolymers AB and BC or AB and CD [30–32]. For example, Jerome et al. prepared CSC micelles with a pH-responsive shell from polystyrene-*b*-poly(2-vinyl pyridine)-*b*-poly(ethylene oxide) (PS-*b*-P2VP-*b*-PEO) [25]. Our group reported a thermo- and pH-responsive triblock copolymer of poly(ethylene glycol)-*b*-poly(4-vinylpyridine)-*b*-poly(*N*-isopropylacrylamide) (PEG-*b*-P4VP-*b*-PNIPAM), which existed as unimers at 25 °C pH 2.0 and self-assembled into CSC micelles with increasing of temperature and pH [26]. So far, double-responsive CSC micelles with responsive shell and corona have been

* Corresponding author. Tel.: +86 22 23501945; fax: +86 22 23503510.
E-mail address: shilinqi@nankai.edu.cn (L. Shi).

0032-3861/$ - see front matter © 2006 Elsevier Ltd. All rights reserved.
doi:10.1016/j.polymer.2006.04.041

scarcely investigated. Understanding the dynamics of these micelles are also important to broaden the potential applications of polymeric micelles.

Very recently, Eisenberg et al. reported on the formation of bowl-shaped aggregates from the self-assembly of an amphiphilic random copolymer of poly(styrene-*co*-methacrylic acid) [P(S-*co*-MAA)], where most of short hydrophilic segments are buried inside the core due to hydrogen bonding; the hydrophobic segments form the continuous matrix and part of hydrophilic segments provide an exterior corona for the aggregates [33]. If the random copolymers consist of responsive segments, the morphology of the aggregates may be more easily adjusted. In this paper, we report the formation of thermo- and pH-responsive CSC micelles from self-assembly of a asymmetric diblock copolymer of poly(*t*-butyl acrylate-*co*-acrylic acid)-*b*-poly(*N*-isopropylacrylamide) [P(*t*BA-*co*-AA)-*b*-PNIPAM].

2. Experimental section

2.1. Materials

1-Chlorophenylethane (1-PECl) (Acros Organics, USA). *t*-Butyl acrylate (*t*BA) (Aldrich, AR) was dried with CaH_2 and then distilled under vacuum. *N*,*N*,*N*′,*N*″,*N*‴-Pentamethyl diethylenetriamine (PMDETA) (AR, Acros Organics, USA). *N*-Isopropylacrylamide (NIPAM) (Acros Organics USA) was purified by recrystallization in benzene/*n*-hexane mixtures and dried in a vacuum. Tris[2-(dimethylamino)ethyl]amine (Me_6-TREN) was synthesized from tris(2-amino)ethyl amine (TREN) (Aldrich) [34]. CuCl was synthesized in our laboratory. Other analytical reagents were used as received.

2.2. Synthesis of block copolymer

The macroinitiator of poly(*t*-butyl acrylate) (P*t*BA-Cl) was prepared according to the published report [35] using 1-PECl as initiator and CuCl/PMDETA as catalyst at 100 °C for 6 h in the mixture solvent of butanone and 2-propanol (7:3 by volume).

Block copolymer of P*t*BA-*b*-PNIPAM was obtained through P*t*BA-Cl initiating polymerization of NIPAM. A typical polymerization procedure is as follows: P*t*BA-Cl (3.0 g) was added to a reaction flask and then 6 mL mixture solvent of butanone and 2-propanol (6:4 by volume) was added. The sample was first stirred and then degassed under nitrogen purge. Subsequently, CuCl and Me_6TREN were introduced into the reaction flask. At last, NIPAM (9.0 g) was added into the flask and degassed under nitrogen purge again. Polymerization was performed at 40 °C for 48 h. The product was purified by passing through Al_2O_3 column and then deposited in a methanol/water mixture.

The block of poly(*t*-butyl acrylate) in copolymers was hydrolyzed to poly(acrylic acid) by using *p*-toluenesulfonic acid as the catalyst in refluxing toluene at 110 °C.

2.3. Characterizations

Molecular weights and polydispersity index (PDI) of P*t*BA-Cl and P*t*BA-*b*-PNIPAM were characterized by a Waters 600E gel permeation chromatography (GPC) analysis system, where THF was used as the eluent and narrow-polydispersity polystyrene as the calibration standard.

The composition of block copolymers before and after hydrolysis was recorded using a Bruker AV300 spectrometer (^{1}H NMR) in $CDCl_3$ or DMSO.

Dynamic laser scattering (DLS) and static laser scattering (SLS) measurements were performed on a laser light scattering spectrometer (BI-200SM) equipped with a digital correlator (BI-10000AT) at 514 nm. The block copolymer P(*t*BA-*co*-AA)-*b*-PNIPAM was directly dissolved in water at room temperature. The copolymer solution with a given pH value was adjusted with HCl and NaOH. All samples with the same concentration of 0.2 mg/mL were first prepared by filtering about 1 mL of the aqueous solution with a 0.45 μ Millipore filter into a clean scintillation vial and heating at a given temperature for about 1 h and then characterized by DLS and SLS.

In DLS measurements, the measured intensity–intensity time correlation function $G^{(2)}(t,q)$ in the self-beating mode can result in a line-width distribution $G(\Gamma)$. For a pure diffusive relaxation, $G(\Gamma)$ is related to the translational diffusion coefficient D by $G(D)$ since $D=\Gamma/q^2$ at $\theta\to 0$ and $C\to 0$ or a hydrodynamic diameter distribution $f(D_h)$ via the Stokes-Einstein equation $D_h=k_bT/(3\pi\eta D)$, where k_b, T, and η are the Boltzmann constant, the absolute temperature and the solvent viscosity, respectively. In the present study, D^0 of the resultant micelles at given concentration is calculated by extrapolating q^2 to 0, and then the hydrodynamic diameter D_h^0 or the hydrodynamic radius R_h^0 and the hydrodynamic diameter distribution $f(D_h)$ at given polymer concentration are calculated.

On the basis of SLS theory, for a given dilute polymer solution at concentration C (g/mL) and at the scattering angle θ, the angular dependence of the excess absolute average scattered intensity, known as the excess Rayleigh ratio $R(\theta,C)$, can be approximated as

$$\left[\frac{KC}{R(\theta,C)}\right]=\left[\frac{1}{M_w}\right]\left[1+\frac{\left(R_g^2q^2\right)}{3}\right] \quad (1)$$

where K is the optical constant and $K=4\pi^2n^2(dn/dc)^2/(N_A\lambda_0^4)$ with N_A, n, λ_0 being Avogadro's number, the solvent refractive index and the wavelength of laser, respectively; dn/dc is the specific refractive index increment, q is the magnitude of the scattering wave vector and $q=(4\pi n/\lambda_0)\sin(\theta/2)$, respectively. After measuring $R(\theta,C)$ at a set of θ, the value of gyration radius R_g and apparent weight-average molecular weight M_W are determined based on the Eq. (1).

The specific refractive index increment (dn/dc) was determined using the Wyatt Optilab DSP interferometric refractometer at a wavelength of 514 nm at 25 °C.

Transmission electron microscopy (TEM) measurement was performed on a Philips EM400ST electron microscopy at

an acceleration voltage of 200 kV. The preparation of samples for TEM was performed in an oven at constant temperature of 25 or 50 °C, respectively. For the observation of the micelles, the micellar solution was first heated at a given temperature, and then a drop of the solution was deposited onto a preheated carbon-coated copper EM grid, and dried at the same temperature at atmospheric pressure.

3. Results and discussion

3.1. Synthesis and characterization of P(tBA-co-AA)-b-PNIPAM

Utilizing ATRP, the P*t*BA-Cl macroinitiator with lower polydispersity successfully initiated the second block to obtain diblock copolymer of P*t*BA-*b*-PNIPAM. The synthesis procedures are illustrated in Scheme 1. The molecular weight and PDI of P*t*BA-Cl and P*t*BA-*b*-PNIPAM are shown in Table 1.

The composition of the block copolymers and the degree of hydrolysis of *tert*-butyl groups to carboxyl are determined from ^{1}H NMR. Fig. 1 shows the ^{1}H NMR spectra of P*t*BA-Cl, P*t*BA-*b*-PNIPAM and P(*t*BA-*co*-AA)-*b*-PNIPAM. In Fig. 1(A) and (B), the sharp resonance at 1.4 is attributed to the $-C(CH_3)_3$ of the P*t*BA block. The chemical shifts at about 1.1 and 4.0 in Fig. 1(B) are attributed to the methyl and methine protons of the PNIPAM block, respectively. The ^{1}H NMR results are thus consistent with the structure of P*t*BA-*b*-PNIPAM. The composition of the block copolymer given in Table 1 is determined by the ratio of characteristic

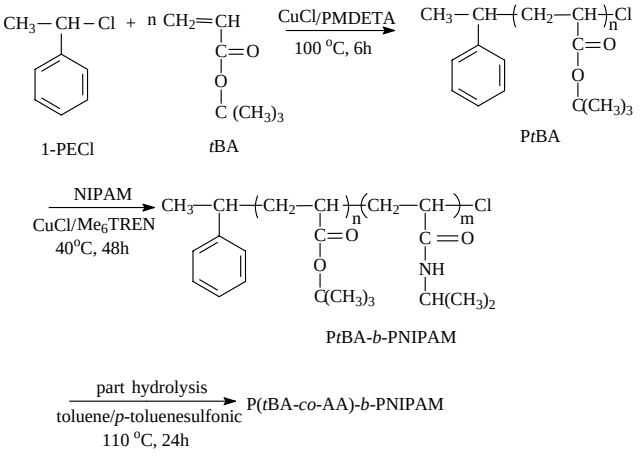

Scheme 1. Synthesis of P(*t*BA-*co*-AA)-*b*-PNIPAM.

Table 1
Characteristics of P*t*BA and P*t*BA-*b*-PNIPAM

Sample	M_n, th (g/mol)	M_n, GPC (g/mol)	PDI	M_n(*t*BA)/M_n(NIPAM) by ^{1}H NMR	Degree of hydrosis
P*t*BA	3.0×10^3	3.80×10^3	1.25		
P*t*BA-*b*-PNIPAM	1.1×10^4	1.06×10^4	1.23	30:68	70%

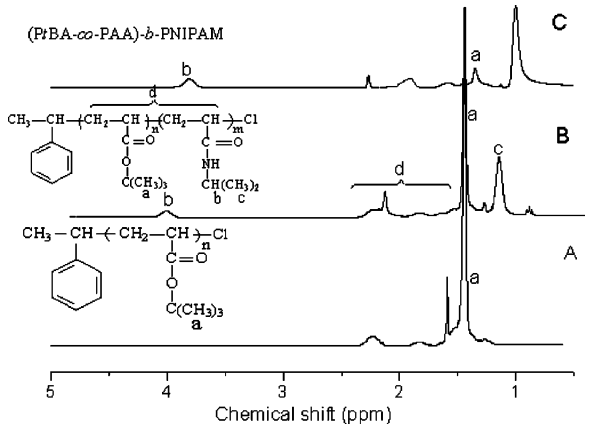

Fig. 1. The ^{1}H NMR spectra of (A) P*t*BA and (B) P*t*BA-*b*-PNIPAM in $CDCl_3$; (C) P(*t*BA-*co*-AA)-*b*-PNIPAM in DMSO.

peaks area of *tert*-butyl protons in P*t*BA blocks and methine protons in PNIPAM blocks (a and b, respectively, in Fig. 1(B)). In Fig. 1(C), the great decrease of the *tert*-butyl resonances at 1.4 indicates the part hydrolysis of P*t*BA into PAA, from which the degree of hydrolysis is determined as 70%.

3.2. Thermo- and pH-responsive core–shell–corona micelles from P(tBA-co-AA)-b-PNIPAM

Fig. 2 shows the plot of the translational diffusion coefficient (D) versus q^2 of P(*t*BA-*co*-AA)-*b*-PNIPAM micelles at pH 5.8 and 25 °C. From the fitted line in Fig. 2, the translational diffusion coefficient D^0 calculated by extrapolating q^2 to 0 at a polymer concentration of 0.20 mg/mL is 5.76×10^{-8} cm^2/s. The translational diffusion coefficient D of the micelles is almost a constant when q^2 increases from 1.544×10^{10} to 8.66×10^{10} cm^{-2} (or θ from 45 to 130°), which suggests the micelles are spherical. The hydrodynamic diameter D_h of the micelles is 79.6 nm according to Stokes–Einstein equation. The hydrodynamic diameter distribution $f(D_h)$ of the P(*t*BA-*co*-AA)-*b*-PNIPAM micelles is inserted in

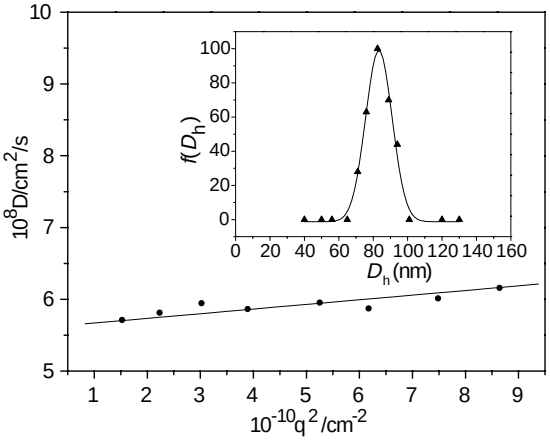

Fig. 2. Plot of the translational diffusion coefficient D versus q^2 of P(*t*BA-*co*-AA)-*b*-PNIPAM micelles at pH 5.8 25 °C.

Fig. 2, which suggests the D_h of the micelles is very narrowly distributed. Considering the block copolymer molecular weight, D_h of the micelles is much larger than simple core–shell structures. This is attributed to the intermolecular hydrogen bonding between PAA and PNIPAM in aqueous solutions at room temperature. In other literatures, hydrogen-bonded interpolymer complexes between poly(acrylic acid) and poly(acrylamide) derivatives have been reported [22,36].

Fig. 3 shows the Berry plots of $[I^{-1}]^{0.5}$ versus q^2 of P(*t*BA-*co*-AA)-*b*-PNIPAM micelles at pH 5.8 and 25 °C, where I is the scattering intensity of the sample at a scattering angle θ. From the fit lines in Fig. 3, the R_g value of the micelles is calculated to be 39.8 nm according to $R_g = (6S/T)^{0.5}$, where S is the slope and T is the intercept of the fit line. The R_g/R_h value can reveal the morphology of particles dispersed in solution [37]. Thus, the R_g/R_h value of P(*t*BA-*co*-AA)-*b*-PNIPAM micelles is 1.01, which is much larger than that of a uniform sphere (~0.775). This suggests the structure of the micelles is incompact due to the longer hydrophilic PAA and PNIPAM segments and the relatively short hydrophobic segments.

In contrast to bowl-shaped aggregates self-assembled from the random copolymer of P(S-*co*-MAA) [33], P(*t*BA-*co*-AA)-*b*-PNIPAM micelles with short hydrophobic segments in this case should have a core–shell structure. Since water is a good solvent for PNIPAM and PAA but a poor solvent for P*t*BA at room temperature, the hydrophobic P*t*BA segments will associate with each other to form a dense core protected by the longer soluble PAA/PNIPAM segments. Considering PAA and P*t*BA chains are randomly distributed, a little fraction of PAA chains may be entangled in the core. But most of PAA chains will stretch outside forming the shell, where some chains may form small loops. Micellization of P(*t*BA-*co*-AA)-*b*-PNIPAM is shown in Scheme 2.

Fig. 4 shows the temperature dependence of hydrodynamic diameter D_h of P(*t*BA-*co*-AA)-*b*-PNIPAM micelles when the polymer solution was heated for about 1 h at each temperature. With increasing temperatures from 25 to 50 °C, water progressively becomes a poor solvent for PNIPAM

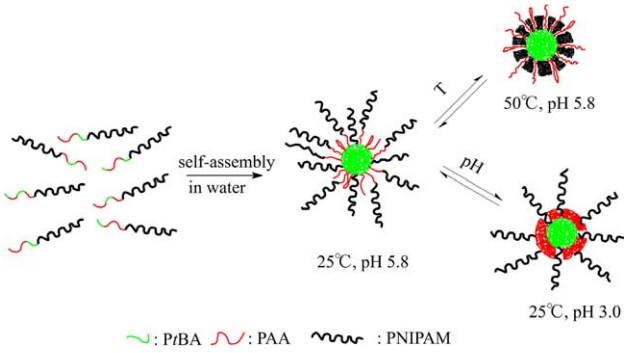

Scheme 2. Schematic illustration of the thermo- and pH-responsive micellization of P(*t*BA-*co*-AA)-*b*-PNIPAM.

blocks so that the stretched PNIPAM chains collapse onto the core leading to the great decrease of D_h from 79.6 to 49.9 nm. The critical aggregation temperature of the copolymer is about 32.4 °C calculated from Fig. 4. When the temperature is above 35 °C, D_h approaches a constant value indicating the shrinkage of PNIPAM blocks stops and a new structure of micelles formed. The hydrodynamic diameter distribution $f(D_h)$ of the micelles formed at 50 °C is shown as an insert in Fig. 4, which is much narrower than that of micelles formed at 25 °C. No precipitation was observed with increasing temperatures further confirms the fact that PAA chains are in the outside shell, if not, the micelles will precipitate with PNIPAM alone as the shell at high temperatures.

Temperature dependence of R_g is shown in Fig. 5(A). The sharp decrease of R_g from 39.8 to 15.9 nm with increasing temperatures from 25 to 50 °C reflects the collapse of PNIPAM chains from an extended coil conformation to a collapsed conformation. The values of R_g/R_h at different temperatures are also calculated as shown in Fig. 5(B). The fact that R_g/R_h values decrease from 1.01 to 0.64 at the temperature above 32 °C clearly reveals the structure of the micelles has changed much from a loose state to a compact state. The R_g/R_h values are lower than that of the uniform solid sphere (~0.775) at high temperatures, which is related to the structure of the micelles with an uneven density distribution [37].

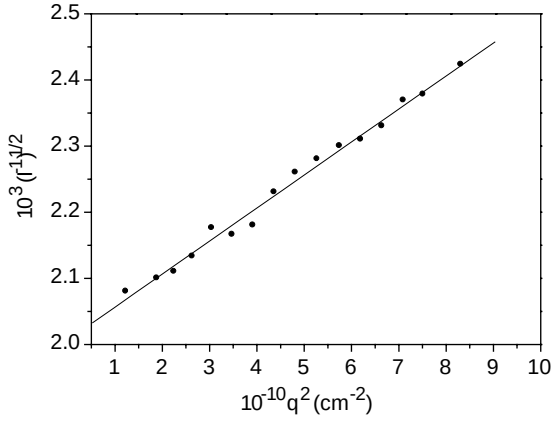

Fig. 3. Berry plot of $[I^{-1}]^{0.5}$ versus q^2 of P(*t*BA-*co*-AA)-*b*-PNIPAM micelles at pH 5.8 25 °C.

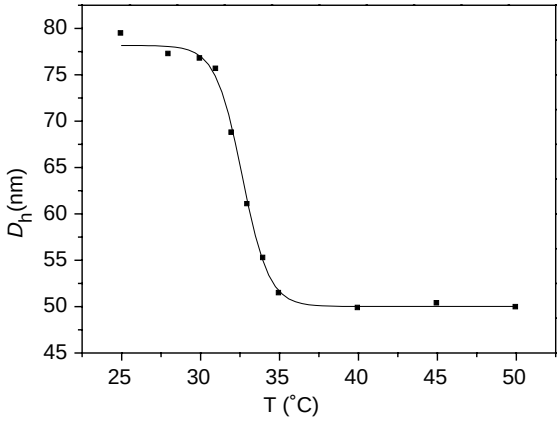

Fig. 4. Temperature dependence of hydrodynamic diameter D_h of P(*t*BA-*co*-AA)-*b*-PNIPAM micelles at pH 5.8 measured at scattering angle 90°.

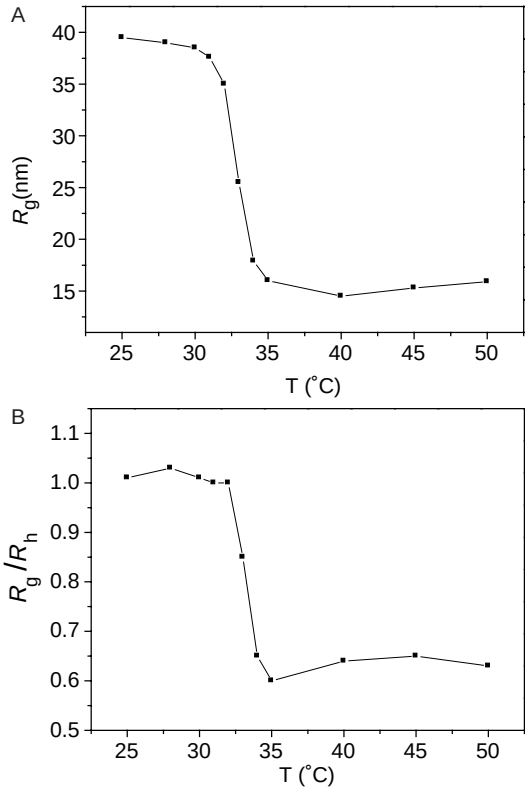

Fig. 5. Temperature dependence of R_g (A) and R_g/R_h (B) of P(*t*BA-*co*-AA)-*b*-PNIPAM micelles at pH 5.8.

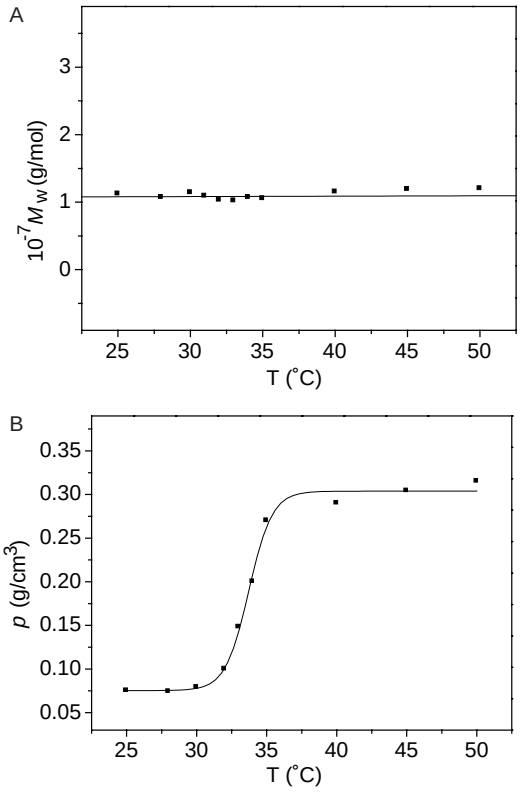

Fig. 6. Temperature dependence of apparent weight-average molar mass M_W (A) and polymer chain density ρ (B) of P(*t*BA-*co*-AA)-*b*-PNIPAM micelles at pH 5.8.

To have a better view of the conformational change, we studied the temperature dependence of the apparent weight-average molar mass M_W and the polymer chain density ρ of P(*t*BA-*co*-AA)-*b*-PNIPAM micelles. The temperature dependence on d*n*/d*c* of the block copolymer has been observed to be minimal [38]. The M_W value of micelles is shown in Fig. 6(A). The apparent M_W of the micelles is nearly unchanged during the increase of temperatures, which means the aggregation number N_{agg} of the micelles is constant based on the equation $N_{agg} = M_{W,micelle}/M_{W,polymer}$. This further confirms the shrinking process of PNIPAM blocks indeed involves only inside the micelles from the corona to the shell. Besides, the polymer chain density is shown in Fig. 6(B) calculated as $\rho = M_{W,micelle}/(N_A\pi/6D_h^3)$. With increasing temperatures from 25 to 50 °C, the ρ value of the micelles increases from 0.075 to 0.31 g/cm^3, indicating the structure of micelles becomes more and more dense.

Fig. 7 shows the TEM images of P(*t*BA-*co*-AA)-*b*-PNIPAM micelles at pH 5.8, 50 °C. The shapes of the micelles were observed as spherical and the diameters are about 30 nm. It must be noted that the D_h of the micelles measured by DLS are a little larger than those observed by TEM. This is because the micelles are swollen in water due to the soluble PAA segments, while TEM observation shows the diameter of the dried micelles [26].

From above discussion, we conclude that core–shell micelles of P(*t*BA-*co*-AA)-*b*-PNIPAM convert into narrowly distributed, CSC micelles at high temperature with hydrophobic P*t*BA as the core, the collapsed PNIPAM blocks as the shell and soluble PAA as the corona. The dense core of micelles is uniformly surrounded by the collapsed PNIPAM, while, hydrophilic PAA chains adjusting their conformation stretch outside to stabilize the micelles. Thermo-responsive CSC micelles of P(*t*BA-*co*-AA)-*b*-PNIPAM is illustrated in Scheme 2. It is worth noting that PAA chains stretching outside the micelles are attached to the P*t*BA core leading to channels throughout the shell. The solubility of PAA chains depends on the degree of ionization, so the size of channels can be tuned by varying pH of the solutions. This system may

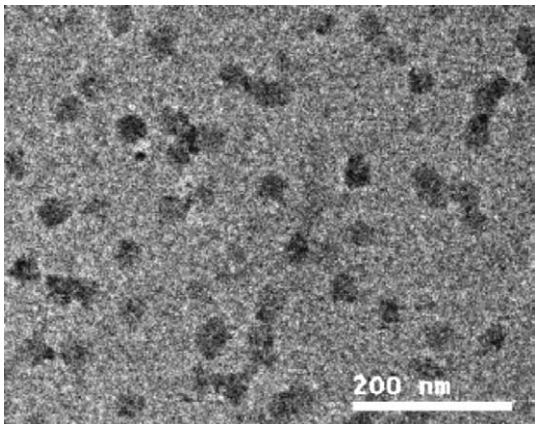

Fig. 7. TEM image of P(*t*BA-*co*-AA)-*b*-PNIPAM micelles at pH 5.8, 50 °C.

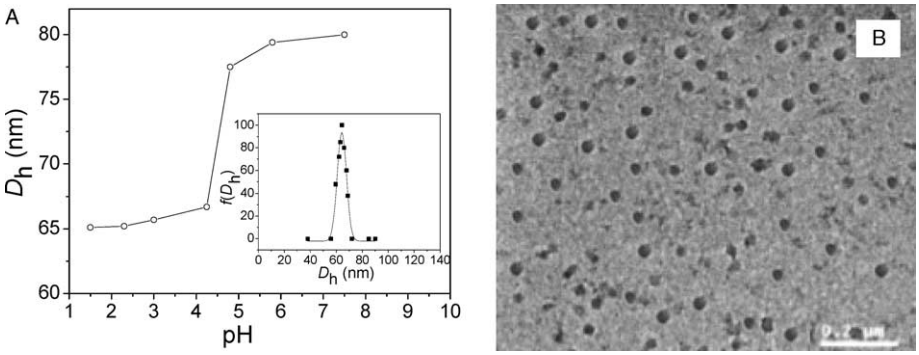

Fig. 8. pH Dependence of hydrodynamic diameter D_h of P(*t*BA-*co*-AA)-*b*-PNIPAM micelles (A) and TEM image of micelles at pH 3.0 (B) at 25 °C.

provide innovative applications in delivery of water-soluble molecules and exchanging of substance.

The P(*t*BA-*co*-AA)-*b*-PNIPAM micelles containing a pH-sensitive PAA shell, can also give response to pH changes of the solution. Fig. 8(A) shows the values of the hydrodynamic diameter D_h of the P(*t*BA-*co*-AA)-*b*-PNIPAM micelles at different pH. It is clear that D_h of the micelles decreases abruptly with the decrease of pH values from 5.0 to 4.2 due to the protonation of carboxylic groups of PAA chains. In the range of pH values from 5.0 to 7.5 and 1.5 to 4.2, D_h of the micelles increases slightly with increasing pH, which is ascribed to the solubility of PAA chains gradually enhanced with the increase of pH values.

The hydrodynamic diameter distribution $f(D_h)$ of the micelles at pH 3.0 and 25 °C is inserted in Fig. 8(A), suggesting the D_h of the micelles is very narrowly distributed. Gyration radius R_g of the micelles at pH 3.0 and 25 °C is 30.2 nm measured from LLS. Thus, the R_g/R_h value is calculated to be 0.92. The decrease of D_h, R_g and R_g/R_h of P(*t*BA-*co*-AA)-*b*-PNIPAM micelles at low pH confirms the conformational change of PAA chains from extended forms to shrunken forms. The resultant micelles are expected to have a CSC structure with hydrophobic P*t*BA segments as the core, the collapsed PAA segments as the shell and soluble PNIPAM segments as the corona. TEM image of (P*t*BA-*co*-PAA)-*b*-PNIPAM micelles at pH 3.0 and 25 °C is shown in Fig. 8(B) suggesting the micelles are spheres and the diameters are consistent with the DLS results.

4. Conclusions

Thermo- and pH-responsive CSC micelles with different structures are formed from self-assembly of a new type of asymmetric diblock copolymer of P(*t*BA-*co*-AA)-*b*-PNIPAM. To our knowledge, this is the first report on the CSC micelles with a responsive shell and corona. At pH 5.8 and 25 °C, P(*t*BA-*co*-AA)-*b*-PNIPAM self-assembles into core–shell micelles with hydrophobic P*t*BA segments as the core, hydrophilic PAA/PNIPAM segments as the mixed shell. Increasing temperatures or decreasing pH values, the micelles convert into CSC structures with P*t*BA as the core, collapsed PNIPAM or collapsed PAA as the shell and soluble PAA or soluble PNIPAM as the corona. These CSC micelles may be useful in a variety of applications.

Acknowledgements

The financial support by Outstanding Scholar Program of Nankai University, National Science Foundation of China (No. 50273015, 20474032 and 23030407) is gratefully acknowledged.

References

[1] Bergbeiter DE, Koshti N, Franchina JG, Frels JD. Angew Chem, Int Ed 2000;39:1040.
[2] Haag R. Angew Chem, Int Ed 2004;43:278.
[3] Shen H, Zhang L, Eisenberg A. J Am Chem Soc 1999;121:2728.
[4] Fujii S, Cai Y, Weaver JVM, Armes SP. J Am Chem Soc 2005;127:7304.
[5] Zhu PW, Napper DH. Macromolecules 1999;32:2068.
[6] Du J, Armes SP. J Am Chem Soc 2005;127:12800.
[7] Jiang J, Tong X, Zhao Y. J Am Chem Soc 2005;127:8290.
[8] Szczubialka K, Nowakowska M. Polymer 2003;44:5269.
[9] Sugihara S, Kanaoka S, Aoshima S. J Polym Sci, Part A: Polym Chem 2004;42:2601.
[10] Kuckling D, Adler H-JP, Arndi K-F. Macromol Chem Phys 2000;201:273.
[11] Huang J, Wu X. J Polym Sci, Part A: Polym Chem 1999;37:2667.
[12] Zhang W, Zhou X, Li H, Fang Y, Zhang G. Macromolecules 2005;38:909.
[13] Zhang W, Shi L, Wu K, An Y. Macromolecules 2005;38:5743.
[14] Wintgens V, Charles M, Allouache F, Amiel C. Macromol Chem Phys 2005;206:1853.
[15] Hofkens J, Hotta J, Sasaki K, Masuhara H, Taniguchi T, Miyashita T. J Am Chem Soc 1997;119:2741.
[16] Zhu X, DeGraaf J, Winnik FM, Leckband D. Langmuir 2004;20:10648.
[17] Kujawa P, Segui F, Shaban S, Diab C, Okada Y, Tanaka F, et al. Macromolecules 2006;39:341.
[18] (a) Liu F, Eisenberg A. J Am Chem Soc 2003;125:15059.
(b) Zhang L, Eisenberg A. Macromolecules 1996;29:8805.
[19] Teoh SK, Ravi P, Dai S, Tam KCJ. Phys Chem B 2005;109:4431.
[20] Andre X, Zhang M, Muller AHE. Macromol Rapid Commun 2005;26:558.
[21] Liu S, Billingham NC, Armes SP. Angew Chem, Int Ed 2001;40:2328.
[22] Schilli CM, Zhang M, Rizzardo E, Thang SH, Chong YK, Edwards K, et al. Macromolecules 2004;37:7861.
[23] Lee RS, Li HR, Yang JM, Tsai FY. Polymer 2005;46:10718.
[24] Ravi P, Dai S, Hong KM, Tam KC, Gan LH. Polymer 2005;46:4714.
[25] (a) Gohy J-F, Willet N, Varshney S, Zhang JX, Jerome R. Angew Chem, Int Ed 2001;40:3214.

(b) Lei L, Gohy J-F, Willet N, Varshney S, Zhang JX, Varshney S, et al. Macromolecules 2004;37:1089.
(c) Lei L, Gohy J-F, Willet N, Zhang JX, Varshney S, Jerome R. Polymer 2004;45:4375.
[26] Zhang W, Shi L, Ma R, An Y, Xu Y, Wu K. Macromolecules 2005;38:8850.
[27] Liu S, Weaver JVM, Tang Y, Billingham NC, Armes SP. Macromolecules 2002;35:6121.
[28] Dimitrov P, Porjazoska A, Novakov CP, Cvetkovska M, Tsvetanov CB. Polymer 2005;46:6820.
[29] Zhu J, Yu H, Jiang W. Polymer 2005;46:11962.
[30] Talingting RM, Munk P, Webber SE. Macromolecules 1999;32:1593.
[31] Pergushov DV, Remizova EV, Gradzielski M, Lindner P, Feldthusen J, Zezin AB, et al. Polymer 2004;45:367.
[32] Zhang W, Shi L, Gao L, An Y, Wu K. Macromol Rapid Commun 2005;26:1341.
[33] (a) Liu X, Kim J-S, Wu J, Eisenberg A. Macromolecules 2005;38:6749.
(b) Liu X, Wu J, Kim J-S, Eisenberg A. Langmuir 2006;22:419.
[34] Ciampolini M, Nardi N. Inorg Chem 1966;5:41.
[35] Davis KA, Matyjaszewski K. Macromolecules 2000;33:4039.
[36] Shibanuma T, Aoki T, Sanui K, Ogata N, Kikuchi A, Sakurai Y, et al. Macromolecules 2000;33:444.
[37] Tu Y, Wan X, Zhang D, Zhou Q, Wu C. J Am Chem Soc 2000;122:10201.
[38] Qiu X, Wu C. Macromolecules 1997;30:7921.